Engineering Geology 312 (2023) 106950

Contents lists available at ScienceDirect

Engineering Geology

journal homepage: www.elsevier.com/locate/enggeo

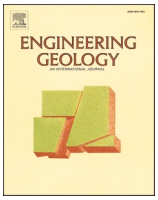

Probabilistic estimation of tunnel inflow from a karstic conduit network

Valentin Dall'Alba [a,1,*], Alexis Neven [a,1], Rob de Rooij [b], Marco Filipponi [d], Philippe Renard [a,c]

[a] Centre of Hydrogeology and Geothermics, University of Neuchâtel, Neuchâtel, Switzerland
[b] Water Institute, University of Florida, 570 Weil Hall, PO Box 116601, Gainesville, FL32611-6601, USA
[c] Department of Geosciences, University of Oslo, Oslo, Norway
[d] National Cooperative for the Disposal of Radioactive Waste (NAGRA), Wettingen, Switzerland

ARTICLE INFO

Keywords:
Karst
Prediction of karst water inflow
Tunnel construction
Stochastic simulations
DisCo
Pykasso

ABSTRACT

When planning infrastructures such as tunnels in karstified formations, a risk assessment of groundwater inflow must be conducted. The aim of this paper is to present a workflow for the probabilistic estimation of the water inflow from karst conduits using a Monte-Carlo approach. The procedure involves three main steps. First, realistic stochastic karstic conduit network geometries are generated based on fracture and stratigraphic information using the Stochastic Karstic Simulation approach (SKS). To represent the geological uncertainty, different scenarios are considered. Then, a discrete–continuum numerical modeling approach is employed, allowing the flow calculation to account for the exchange between the matrix and the conduits as well as the transition between turbulent and laminar flow in the conduits. Because it is not known if and where (at which depths) the tunnel may hit a karst conduit, and what will be the pressure gradient in the system, different hydrogeological scenarios are considered in the uncertainty analysis phase including a randomized location of the tunnel, a range of possible pressure gradients, and a range of possible matrix permeability values. The final step consists of the statistical analysis of the results. The proposed workflow allows estimating the range of plausible inflows and studying how the inflows are related to the network geometry properties and to the hydrodynamic parameters of the aquifer. This method is illustrated in a simple synthetic but realistic case of a rather deep and confined karstic formation. In that situation, the results show that even if the pressure difference in the system and the matrix permeability value are important factors controlling the long-term inflow, the karstic conduit network geometry and connectivity also play a critical role in the determination of the potential discharge. Overall, this study demonstrates the possibility and advantages of using stochastic analysis in the early phases of project planning to predict possible long-term water inflow in tunnel after its construction.

1. Introduction

Karstic aquifers are generally made of a rather low-permeability fractured matrix and of networks of highly permeable conduits (Ford and Williams, 2007; Goldscheider and Drew, 2014). These aquifers present a large spatial heterogeneity. The density of the karst conduit depends on many factors such as lithology, hydrological conditions, the morphology of the catchment, topographical gradient, possible locations of the outlets, the density of fracturation, etc. Hydrologically speaking, the hydraulic head in the system and the discharge rates can vary extremely rapidly in space and time, with some parts of the conduit network being only active under specific hydrological conditions.

Due to their heterogeneous nature, their poor predictability, and their ability to conduct water very rapidly, karstified rock masses are among the most risky environments when planning underground constructions such as tunnels. When excavating a tunnel or a mine in these environments, an important risk is to cross a karst conduit and flood the tunnel with fast and massive water inflow (Day, 2004). Such events can be devastating for the infrastructure and extremely dangerous for the personnel. In addition, when these rapid changes occur, the drainage can cause collapse or subsidence at the surface (Song et al., 2012; Gutiérrez et al., 2014; Lee and Moon, 2020) and drying up of springs (Vincenzi et al., 2013; Jeannin et al., 2015). These effects can also have major ecological impacts on vegetation or wetlands at the surface (Liu et al., 2019; Lv et al., 2020). Obviously, the consequences of all these issues can be very significant, inducing large delays and additional costs

* Corresponding author.
E-mail address: valentin.dallalba-arnau@unine.ch (V. Dall'Alba).
[1] These authors contributed equaly as first author

https://doi.org/10.1016/j.enggeo.2022.106950
Received 15 March 2022; Received in revised form 19 August 2022; Accepted 22 November 2022
Available online 28 November 2022
0013-7952/© 2022 The Authors. Published by Elsevier B.V. This is an open access article under the CC BY license (http://creativecommons.org/licenses/by/4.0/).

on the projects, if not a more dramatic situation involving casualties.

Water inflows in tunnels are frequent. They can occur from localized high permeability zones or from fractures. However, karst-related water inrushes are usually several orders of magnitude higher. We can also differentiate two types of karst-related water arrival into tunnels. The first one, linked to more extreme events, is due to the initial burst of water when crossing a filled karst conduit. The second one is related to the long-term inflow that can be expected from the karst conduit once the first burst has passed and the steady-state has been reached. The difference in water flow between these two events can be extremely large. In this study, we are focusing on the estimation of the second one, the long-term inflow.

To evaluate and predict karst-related water arrivals into tunnels, a wide variety of methods exists. The simplest are analytical formulas derived for circular tunnels in an effective porous medium in steady-state (Chisyaki, 1984; El Tani, 2003; Raymer, 2005; Butscher, 2012) or transient regime (Perrochet, 2005; Renard, 2005; Hwang and Lu, 2007; Maréchal et al., 2014). It is also possible to use simple rainfall-runoff models (Luo et al., 2022). All these solutions do not consider explicitly the presence of karst conduits. Xie et al. (2019) and Jiang et al. (2021) proposed to account for the presence of karst conduits by considering a semi-infinite porous matrix, a circular tunnel, and a circular karst conduit fully saturated and running parallel to the tunnel at a certain distance. The flux is going through the rock matrix and the tunnel is not supposed to hit the karst conduit. A few authors consider a fractured matrix and model it with an effective permeability tensor or a double porosity approach (Maleki, 2018; Sedghi and Zhan, 2021). Again, none of these methods account for the scenario in which a conduit is directly crossed by the tunnel during its construction.

To predict the water inflow in the situation where a tunnel hits a karst conduit, one possibility is to employ the Darcy–Weisbach equation to estimate the groundwater flux through a pipe, representing the main karst conduit, and connecting a recharge area with the tunnel (Çengel and Cimbala, 2017). The advantage of this approach is that it accounts for the turbulent flow in the pipe, which is normally ignored when working with a porous matrix approach. However, one main difficulty with this approach is estimating the friction factor and the geometric parameters at the scale of the aquifer. The friction factors are known to depend on the Reynolds number and on the rugosity of the conduits. A review of regional friction factor values estimated on karstic conduit networks was published by Herman et al. (2012). These values cover a wide range from 0.1 to 340 (dimensionless coefficient), while the friction factors estimated using the Colebrook formula and the theory of flow through pipes are much smaller (between 0.03 and 0.9) according to Herman et al. (2012). Therefore, applying such a simple analytical solution poses a challenge in terms of determining a proper parameter's value.

An alternative approach is to construct a numerical model representing the geology of the site and modeling the system using an equivalent porous or fractured media (Javadi et al., 2016; Scheidler et al., 2017; Park et al., 2020; Li et al., 2021). As for the analytical solutions, these evaluations of tunnel inflows do not explicitly account for karst conduits. They generally calibrate the parameters of the model based on field data to represent globally the underground. Only a few studies did model explicitly the karst conduits to assess the hazards related to tunneling. He (2015) models the burst of water from a large fully saturated cavity directly into the tunnel at the scale of a few seconds to several minutes after the accident. Jeannin et al. (2015) represent the karstic aquifer at a broader spatial and temporal scale, where the geometry of the conduits was estimated based on the interpretation of a 3D structural geological model of the area, in situ speleological observations, and applied speleogenetic principles. The flow in the conduits was modeled using the Storm Water Management Model (SWMM) code without explicitly representing the matrix but accounting for complex activation of different parts of the conduit network depending on its degree of saturation and accounting for complex recharge processes.

Other articles developed global methodologies to estimate the hazards related to karst features when tunneling (Filipponi and Jeannin, 2010; Li et al., 2013; Lin et al., 2020). These authors couple the analysis of multiple factors and often combine them to evaluate a hazard index. Stochastic methods are rarely described in publications. One recent example is the paper of Gangrade et al. (2021), which describes the use of a plurigaussian geostatistical simulation technique to model the hazards of encountering karst voids for a planned tunnel project.

In this paper, we present a methodology for the probabilistic prediction of groundwater long-term inflow from a karstified formation into a tunnel. We approach the problem using a combination of statistical methods and physically-based modeling approaches. The statistical model allows to account for the various sources of uncertainty that are affecting the analysis, and the physically-based approach allows to rely as much as possible on sound physical theories. This type of stochastic approach to evaluate risks in karstic environments has been pioneered by Jaquet et al. (2004) who combined a stochastic model based on the Langevin equation to generate the karst network geometry and a physically based flow simulation tool. The methodology introduced in this paper follows a similar general workflow. To quantify the uncertainty and obtain the probability distribution of the inflows, a Monte-Carlo analysis is conducted. An ensemble of models representing the karstic system is generated and for each model, an inflow is estimated. The three main steps are 1) the stochastic simulation of karstic conduit network geometries, 2) the stochastic simulation of conduit diameters, and 3) the simulation of groundwater flow in the karstic system. Compared to the workflow proposed by Jaquet et al. (2004), the approach presented in this paper differs for each of these steps. The conduit geometry is obtained using the Stochastic Karst Simulation (SKS) pseudo-genetic approach introduced by Borghi et al. (2012) instead of the Langevin method of Jaquet et al. (2004). The advantage of the SKS approach is that it can be used to integrate easily prior geological and hydrological information available on site. For the simulation of the conduit diameters, we use a geostatistical simulation method similar to the one proposed by Pardo-Igúzquiza et al. (2012). Again the advantage is that we can constrain the simulations by statistical data available in the zone of interest. And finally, for the flow simulation we use the recent *DisCo* code that is capable of handling complex karst networks embedded in a permeable matrix (De Rooij et al., 2013; De Rooij, 2019). The code uses a well-index to describe efficiently the exchanges between the matrix and the conduits, and it accounts both for laminar and turbulent flow. The combination of all these novel features should permit obtaining more robust and reliable estimates of risks when designing tunnels in karstic formations.

This work focuses on the estimation of the possible long-term/steady-state water inflow in a tunnel excavated through a confined karstified rock mass in a simplified situation. Finally, we also compare this approach with a much simpler one based on the analytical solution corresponding to a single pipe and discuss how this solution should be parameterized.

The paper is structured as follows. The first section presents the details of the implementation of the method and the geological assumptions that were made to illustrate the approach. The next section illustrates the type of results that one can obtain with such an approach and the last section discusses the advantages and limitations of the method.

2. Physically-based stochastic estimation of tunnel inflows

In this section, we first introduce an overview of the proposed methodology, present the simplified case study, and then explain the details of all the steps.

2.1. Overview of the methodology

The aim of the proposed methodology is to estimate the long-term discharge that could happen if a tunnel would hit directly a karst conduit within the phreatic zone of a karstic aquifer and quantify the associated uncertainty. One key motivation for the proposed approach is that it is possible today to obtain reasonably accurate estimates of tunnel inflow by simulating groundwater flow in a karstic system using physically-based numerical simulators (e.g. Panday and Huyakorn, 2004; Shoemaker et al., 2008; Reimann et al., 2011; Kresic and Panday, 2018; De Rooij, 2019). However, these numerical techniques require knowing the geometry of the system (3D geology, karst conduits), the petro-physical parameters (permeability, conduit diameters, etc.), and the boundary conditions in order to be able to run the model and get an estimate.

Obviously, when the objective is to estimate a risk, especially in the early stages of the design of a tunnel project, a part of this information is not available. It is impossible to know in advance for example, where the tunnel will hit a karst conduit. This lack of knowledge cannot be completely resolved by acquiring additional data since it is not feasible to measure all the geometrical and petrophysical parameters exhaustively in a complex underground system.

To account for this intrinsic lack of knowledge, we propose to use a classical Monte-Carlo simulation approach. It consists in generating an ensemble of models representing the variety of scenarios that may occur based on local knowledge. In the case of the tunneling project in karstic formation, we consider that the main sources of uncertainty that needs to be represented are 1) the unknown detailed geometry of the karst network, 2) the unknown location at which the tunnel may hit a conduit, and 3) the unknown properties of the conduits (mainly the spatial distribution of the diameter). In any real practical case, other factors may need to be considered depending on the specific geological and hydrogeological conditions of the area. Additional aspects can be added to this general framework. For example, due to the lack of geological data, the 3D position of the karstified formation may not be known accurately and should also be accounted for in the Monte Carlo analysis. The recharge processes or the presence of an unsaturated zone may also be critical factors needing to be studied. All these aspects can be included in the general approach, but for the sake of keeping the paper and example simple, we will focus on the main sources of uncertainty and illustrate how they can be accounted for in a rather simple setup.

In this context, the core of the proposed approach consists in generating an ensemble of models. For each model, the procedure includes the three main steps already presented in the introduction and illustrated in Fig. 1. In step 1, pseudo-genetic karstic conduit networks are generated using the SKS approach implemented within the *Pykasso* code. In step 2, the spatial distribution of the diameters is generated and assigned to the conduits using geostatistical simulations based on observed conduits' aperture distribution. In step 3, the position of the tunnel is sampled and the hydrodynamic simulation of the karstic system is carried out. The hydraulic pressures, velocities, and friction factors are all obtained using the *DisCo* solver. The final step of the methodology is to analyze the statistical distribution of estimated inflows and how it varies with controlling factors.

2.2. Conceptual model for the simplified case study

To illustrate the methodology in a realistic but very simple situation, we assume that a tunnel is planned in a confined karstic formation. The geological context is an undeformed but fractured sedimentary basin with an alternation of aquifers and aquitards. The karstic formation is horizontal and overlaid by an aquifer of considerable water storage. Being at depth, this aquifer is itself confined and overlaid by a succession of other sedimentary formations not represented in the model. Fig. 2a shows a vertical cross-section through this conceptual model. The domain of interest is 2'000 m long and 250 m thick. The bottom and the two lateral sides of the domain are fixed as no-flow boundaries.

The karstic formation (in white in Fig. 2a) is the main target of the study. The tunnel is crossing the section perpendicularly, and we assume that the depth of its construction is not known in advance. The gray layer (in Fig. 2a) represents the saturated porous or densely fractured aquifer that overlays and feeds the karstic aquifer. It is 50 m thick and distributes the groundwater to the karstic aquifer. It is assumed that the amount of water drained by the tunnel when hitting a karst conduit will be small compared to the amount of water stored in all the upper formations and therefore it is considered reasonable to impose a prescribed pressure on the top boundary of the porous formation. In terms of risk analysis, this choice also ensures a safe estimation of the inflows.

The main part of the domain corresponds to the karstic confined aquifer. It is modeled as a two-component system. The fractured rock mass is represented by an equivalent porous matrix with homogeneous hydraulic conductivity. The flow in the matrix is assumed to follow Darcy's law. The second part of the system is the karstic conduit network embedded within the equivalent matrix. The conduit's diameter varies in space, ranging from centimeters to several meters following a specific fixed distribution.

The tunnel is located randomly for each simulation on the karst network. This position represents the tunnel's breached location where a fixed pressure value of zero is prescribed, assuming that the tunnel is connected to the surface and therefore has a pressure close to atmospheric conditions. The pressure difference that is reported in the results corresponds to the pressure difference between the top formation and the tunnel location in the karstic conduit network.

The conceptual model described above and represented in Fig. 2a will be used to construct the numerical model and carry out the Monte-Carlo study. Furthermore, we also consider an even simpler conceptual model where the karstic conduit network is replaced by a single vertical straight pipe (Fig. 2b). This second conceptual model allows one to analytically express the discharge to the tunnel using an equivalent pipe diameter and is compared to the numerical model at the end of this work.

In summary, the main hydrogeological assumptions are the following:

1. The pressure in the tunnel is assumed to be close to the atmospheric conditions and a fixed pressure value of 0 bar is prescribed.
2. The tunnel is going through a limestone rock formation characterized by the presence of karst conduits. It may encounter saturated karst voids with water pressures ranging between 35 and 50 bar.
3. The conduits are supposed to be fed with water from the overlying rock formations and water stored in the fracture network or in the limestone matrix.
4. The flow rate in the tunnel will not be sufficient to dry the overlying reservoir, therefore the karstic aquifer will remain saturated and the top boundary conditions will not be significantly affected.
5. No remediation work is done before or after hitting a karst conduit while simulating the long-term behavior.
6. The karst conduit relative rugosity coefficient is fixed for the entire network at 35%.

2.3. Generation of stochastic karstic conduit networks

The *Pykasso* code [2] (Miville, 2019; Fandel et al., 2021) is used for the generation of the karstic conduit networks geometry. The code is an open-source Python implementation of the Stochastic Karstic Simulation method (SKS) of Borghi et al. (2012).

The method is based on a pseudo-genetic algorithm. The generation of the conduits is iterative and hierarchical and accounts for the heterogeneity of the geological rock formations. The algorithm assumes

[2] https://github.com/randlab/pykasso.

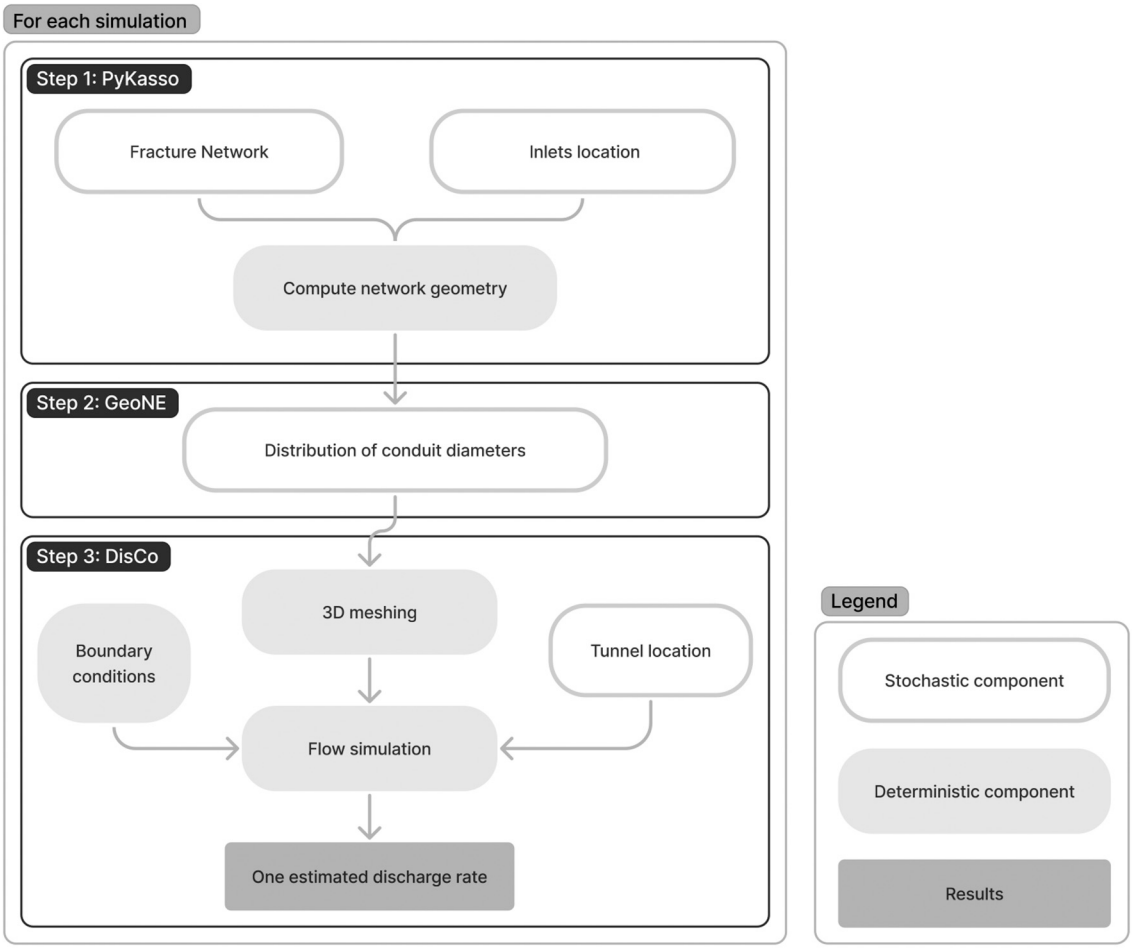

Fig. 1. Schematic illustration of the methodology.

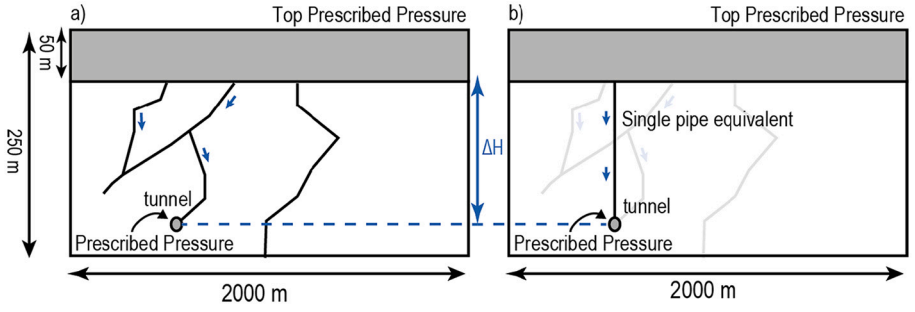

Fig. 2. a) A vertical cross-section through the conceptual model composed of two layers. The top layer is feeding the lower one, where the karstic conduit network and the tunnel breach location are defined. b) Alternative scenario for the single pipe equivalent.

that the development of karst conduits is guided by discontinuities (fractures and bedding planes), which are susceptible to act as preferential dissolution paths (Filipponi et al., 2009; Lowe and Gunn, 1997). The karst development follows the minimum effort path between inlets and outlets along these discontinuities within a 3D geological domain. The geological domain and the discontinuities are represented explicitly. The discontinuities can have fixed locations or can be distributed spatially in a stochastic manner. The paths between inlets and outlets are computed using the fast-marching algorithm (Sethian, 1996). This method has been tested and applied for various sites (e.g. Vuilleumier et al., 2013; Sivelle et al., 2020; Fandel et al., 2020) and has been recently extended to include an anisotropic fast marching algorithm allowing to better account for geometrical information and constraints (Fandel et al., 2021).

The stochastic ingredients in the algorithm are the locations of the inlets and outlets as well as a stochastic discrete fracture network. For each simulation, these features are simulated and a new conduit network is deduced. The algorithm is controlled by a set of parameters, defining the domain that needs to be simulated, the number of inlets/outlets (here we fixed the number of outlet to one), and the statistics of the fracture families. Some initial tests have been conducted to generate conduit networks that would represent some realistic variability and features while remaining sufficiently simple to allow solving the flow equations using their structure.

Two types of network geometrieshave been defined: *Case 1* and *Case 2*. Examples of the resulting conduit networks are displayed in Fig. 3.

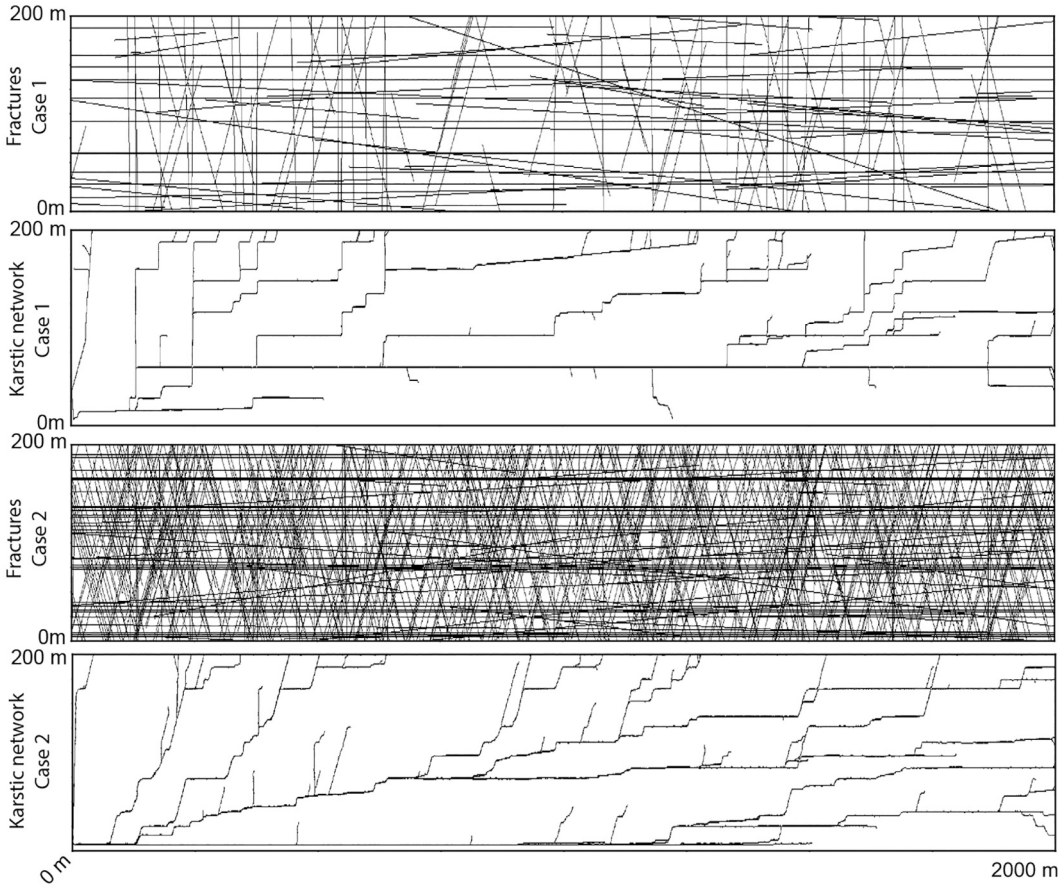

Fig. 3. Example of random fracture networks and the corresponding conduit networks, obtained with Pykasso for *Case 1* and *Case 2*.

Case 1 corresponds to a karstic conduit network with mainly sub-vertical shafts and sub-horizontal karst conduits. In *Case 2* the rock mass is much more fractured resulting in smoother conduit networks when compared to *Case 1*. Most of the karst conduits are either horizontal or slightly inclined, with no deep vertical shafts while they are frequent in *Case 1*. The main parameter used to control the difference of the final aspect is the fracture density. 100 different stochastic geometries have been simulated in total, 50 for each case. The purpose of having two cases is to better cover the uncertainty of the structures of the karstic conduit networks. For a more extensive study or real field applications, additional cases could be included to cover a broader uncertainty space.

The general parameters that have been used to generate these two sets of simulations are presented in Table 1. These main parameters include the dimension of the model domain, the number of fracture families, the position of the outlet (in the bottom left corner), or the coefficient α of the probability distribution function of the length of the fractures. Fractures will act as a preferential development path for the karstic conduit network. The origin of the model ($x = 0$ and $y = 0$) is always defined as being the lower-left corner.

In order to simulate the conduits, *PyKasso* requires inlets to be specified. Inlets are used as starting points for the simulation of the karst conduits and can be spatially located by the user or randomly located by PyKasso. In our model, we differentiated 3 categories of inlets: (1) upper inlets, (2) side inlets, and (3) random inlets. The upper inlets are randomly placed at the top of the model ($y = y\_\max$, $x =$ random) and represent paleo-infiltration points at the top of the model. The side inlets are randomly placed on the side ($y =$ random, $x = x\_\max$) and represent conduits that may come from outside the modeling domain. Finally, inlets are randomly disposed over the whole domain (x & $y =$ random) and represent conduits that may have a "dead end", becoming too small to be considered as a karst conduit. *Pykasso* uses all these points as starting point for the conduits and will follow the minimum effort path toward the outlet. By using these 3 categories together, we ensure a wide diversity of karstic simulations.

In both cases, four families of fractures are defined (Table 2). The main difference is that the fracture density of the two conjugate sets of fractures is much larger in the *Case 2*. In addition to the fractures, we also consider bedding planes. These planes are modeled as horizontal surfaces that are continuous through the domain and are randomly dispatched along the y-axis of the domain.

Table 1
General karstic conduit network simulation parameters used in *Pykasso*.

Parameter	Value
Dimension	2'000 × 200 [m]
Resolution	1 × 1 [m]
Outlet number/ Position	1/ (5,5)
Nb. fractures families	4
Alpha	1.7
Initial Seed	200'000'000

Table 2
Discrete fracture network parameters.

Parameter	Family 1	Family 2	Family 3	Family 4
Fractures min orientation	−5	25	−30	85
Fractures max orientation	5	30	−25	95
Fractures min length	200	100	100	200
Fractures max length	4000	500	500	4000
Fract. densities *Case 1*	10^{-4}	$8{\cdot}10^{-5}$	$8{\cdot}10^{-5}$	10^{-4}
Fract. densities *Case 2*	10^{-4}	$8{\cdot}10^{-4}$	$8{\cdot}10^{-4}$	10^{-4}

2.4. Conduit's diameter simulation

Once the conduit networks are simulated, the next step consists in assigning diameter values to the conduits. Conduit diameters are known to be spatially correlated (Pardo-Iguzquiza et al., 2011; Frantz et al., 2021). To take this into account, unconditional Gaussian random fields (GRF) are employed to simulate the spatial distribution of the diameters. The distribution on which is based the GRF model is derived from an analog distribution of karst conduit sections based on a study site in Switzerland (Fig. 4).

In practice, to assign the diameters, three steps are required for each simulation. First, a Gaussian random field of mean zero and variance one is simulated, with the same extent and resolution as the karstic conduit network model. The covariance model is inspired by the analysis of Pardo-Iguzquiza et al. (2011): it is an anisotropic exponential covariance model with range values fixed at 150 m in the horizontal direction and 50 m in the vertical one. This model reflects the expected spatial continuity of the diameter of the conduit network and is inspired by field observations. Then an inverse normal-score-transform (e.g. Deutsch and Journel, 1992) is applied to the Gaussian field. This step transforms the simulated values into the non-parametric distribution deduced from the measurements collected in Switzerland (Fig. 4). The last step consists in assigning the pixel-wise simulated diameters to the conduits based on the local pixel value. Some examples of the resulting conduit networks with their associated conduit diameters are presented in Fig. 5. For each of the 100 simulated conduit networks, a new simulated GRF is generated and a new conduit's diameter map is constructed.

This procedure has the advantage of being fast and simple and allows to represent the variability of the conduit diameters through the conduit network. It is however a simplification since the conduits are expected to have a stronger spatial correlation along the conduit's extension and not across the 3D Euclidean space in which the conduits are located (Frantz et al., 2021).

2.5. Flow modeling

Following the pioneering work of Király (1976); Király, 1988, discrete-continuum models have been widely used to simulate coupled conduit-matrix flows in karstic systems (e.g. Panday and Huyakorn, 2004; Shoemaker et al., 2008; Reimann et al., 2011; De Rooij et al., 2013; Kresic and Panday, 2018). In such models, the karstic aquifers are represented by interconnected one-dimensional discrete conduit cells embedded within a continuum of three-dimensional matrix cells.

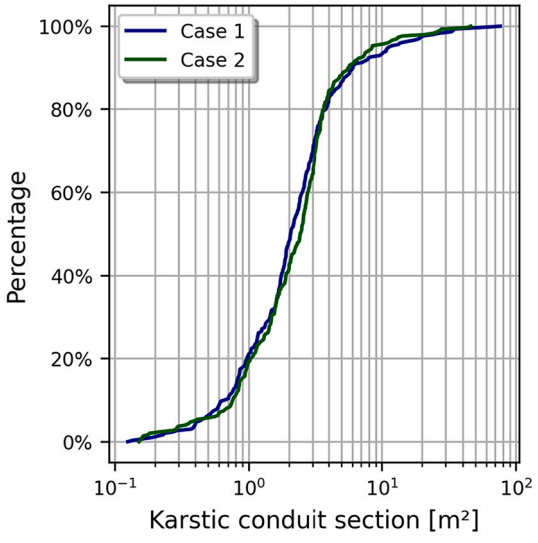

Fig. 4. Cumulative distribution of the assigned area aperture of the modeled karst conduits.

In our workflow, once the karstic conduit networks are generated and conduit diameters are associated, the discrete-continuum model *DisCo* (De Rooij et al., 2013; De Rooij, 2019) is used to estimate the possible long-term inflow at the tunnel location.

In the conduits, the flow velocity can be high and lead to a nonlinear behavior when inertial and turbulent effects become dominant. Even if the transition between laminar and turbulent flow depends on multiple factors, Reynolds established that the dominant parameter was the ratio of inertial forces to viscous forces and introduced the Reynolds Number R_e (Çengel and Cimbala, 2017, p354):

$$Re = \frac{v\rho d}{\mu}, \tag{1}$$

with v the velocity, ρ the density, d the diameter of the conduit, and μ the viscosity. Pipes with a R_e above 4'000 are usually considered under fully turbulent flow. Two main equations are generally used in these conditions, the Manning–Strickler, and the Darcy–Weisbach equations. The Manning–Strickler approach is easier to implement but results in a poorer approximation of the pressure loss, especially when the flow is close to the transition between the laminar and turbulent regimes. The Darcy–Weisbach equation (Çengel and Cimbala, 2017, p.359) is more precise and corresponds to:

$$\Delta H = \frac{v^2}{2g}\frac{\lambda}{d}L, \tag{2}$$

where ΔH is the head loss, g corresponds to the acceleration of gravity, L is the length between the two observation points, and λ is the friction factor. The equation states that the loss of charge along a conduit is proportional to the friction factor λ coefficient, the squared of the velocity value, and the length of the conduit, and inversely proportional to the diameter. The most common way to estimate λ is by using the Colebrook formula (Çengel and Cimbala, 2017). However, this formula is not explicit; the estimation of λ requires using an iterative approach. To avoid such computation, Swamee (1993) proposed an explicit formulation for the friction factor:

$$\lambda = \left\{ \left(\frac{64}{Re}\right)^{8} + 9.5\left[\ln\left(\frac{\epsilon}{3.7d} + \frac{5.74}{R_e^{0.9}}\right) - \left(\frac{2500}{R_e}\right)^{6}\right]^{-16} \right\}^{0.125} \tag{3}$$

with ϵ the surface rugosity. The surface rugosity is linked to the relative rugosity R_r by the diameter such as $\epsilon = R_r \cdot d$. The λ parameter is validated through the full range of the flow regime (laminar to turbulent) and provides a smooth transition between the two domains (Equ. 3). In addition, this equation can be solved directly.

DisCo allows the user to choose between different flow equations and conduit models including the Darcy–Weisbach equation coupled with the Swamee friction factor formulation and is able to switch automatically from one regime to another. The code is based on a finite-difference numerical scheme, and it solves the discrete-continuum problem. Conduit and matrix flows are computed using a robust implicit coupling approach in which the set of discrete conduits and matrix flow equations are solved simultaneously (De Rooij et al., 2013). The exchange flux at the conduit-matrix interface is estimated using a well-index allowing the flux to be less sensitive to the spatial discretization of the matrix cells surrounding the conduits (De Rooij et al., 2013; De Rooij, 2019).

Concerning the setup of the numerical model, the simulations are carried out in a 3D grid composed of 400 cells in the x direction, 50 cells in the z direction and 22 cells in the y direction with a resolution of 5 m on every direction. The first 10 top layers correspond to the zone without karst conduits that acts as a recharge layer for the deeper part of the model (the other 40 layers) in which the conduit network is present (Fig. 6). This two layers model ensures a proper distribution of the inflow in the karstic conduit network on top of the karstified rock

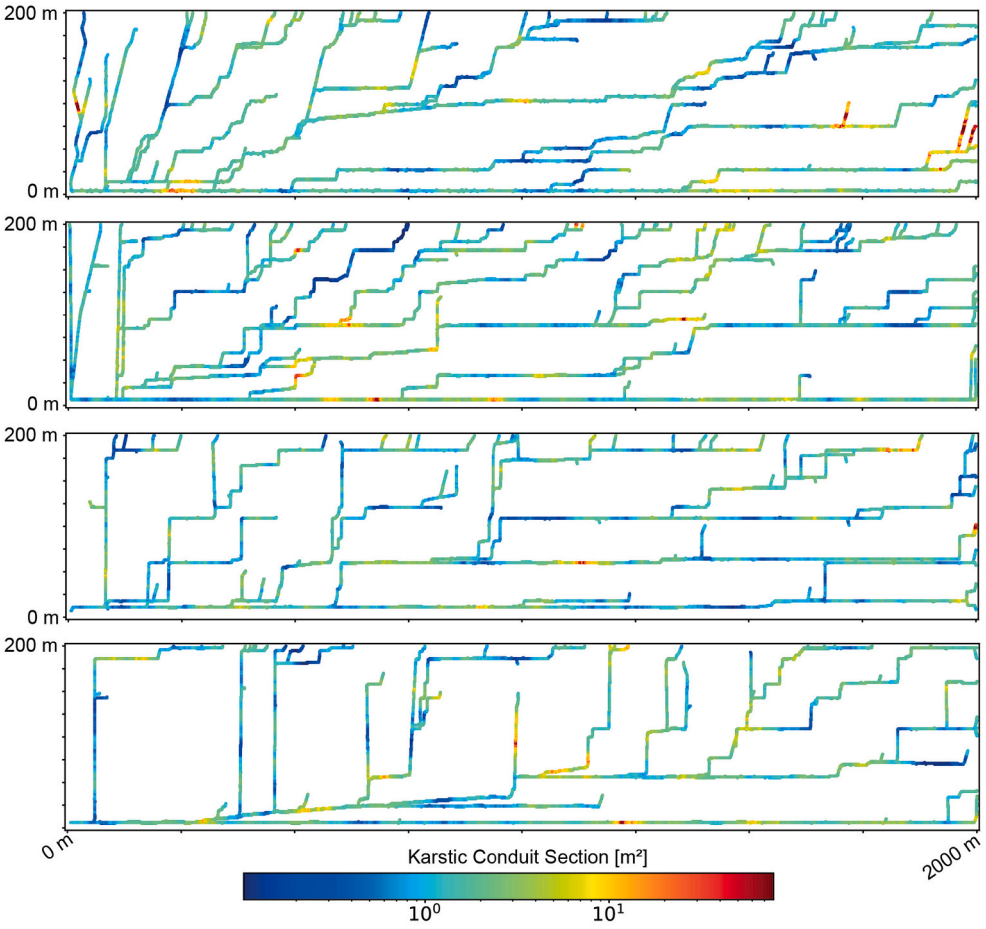

Fig. 5. Example of modeled karstic conduit networks and their associated diameter in log scale.

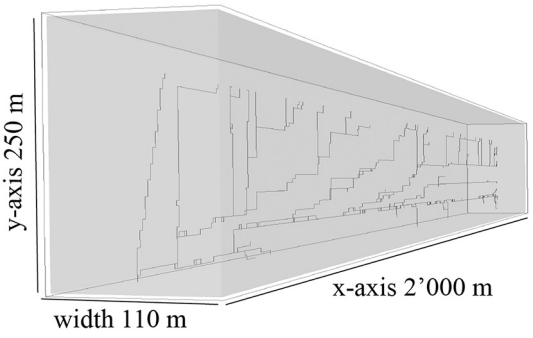

Fig. 6. The modeled karstic conduit network is incorporated in the center layer of the 3D mesh.

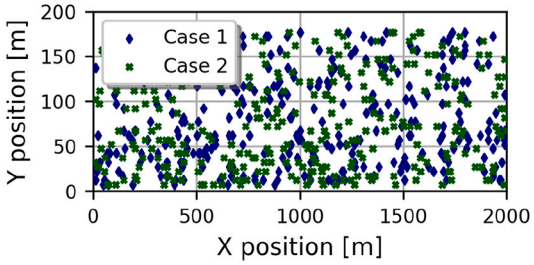

Fig. 7. Tunnel location on the simulation grid through the 600 simulations for both karst scenarios (cross section at y = 55 m).

formation. The conduits are embedded in a three-dimensional matrix and are located in the vertical section located in the middle of the 3D block. This approach allows representing correctly the cylindrical flow that occurs in the matrix around a karst conduit.

To represent the uncertainty related to the location at which the tunnel may hit a karst conduit, 6 different tunnel locations are randomly sampled along each of the 100 conduit networks (50 networks for each karst scenario, *Case 1* and *Case 2*). All these locations are displayed in Fig. 7; they cover a large part of the domain. For each location, a flow solution is computed with *DisCo*. Constant prescribed pressures are fixed on the top of the domain and on the tunnel location to impose a pressure difference corresponding to the maximum estimated pressure. A no-flow condition is assigned to all the other boundaries of the grid.

The results of this work are presented using pressure differences (in bar) between the top layer of the grid and the location of the output of the system (tunnel location = 0 bar). It is important to note that the *DisCo* code works internally with groundwater head values. A conversion factor of 1 bar ≈ 10 m groundwater head value is used.

Three main sets of analyzes are conducted. The first one uses four pressure differences between the top layer and the tunnel location (35, 40, 45, and 50 bar). In these scenarios, the hydraulic conductivity value of the matrix is assumed to be isotropic, homogeneous, and equal to 10^{-7} m/s. In total, 2'400 flow simulations are carried out with this configuration in steady-state, corresponding to 6 tunnel locations for 100 conduit network models and 4 pressure difference set-ups.

The second analysis investigates the influence of the matrix hydraulic conductivity on the long-term inflow. For this test, five matrix hydraulic conductivity values are tested; 10^{-7}, 5.10^{-7}, 10^{-6}, 5.10^{-6} and

10^{-5} m/s. The pressure difference in these cases is fixed at 40 bar and 120 simulations are run for each of these scenarios (6 tunnel locations for 20 networks).

Finally, the results of the simulations are post-processed in the last analysis to evaluate the statistical distributions of the friction coefficients returned by the solver. Both output flow value sets and friction factor results are presented and discussed in the next section.

2.6. Single pipe equivalent

In this section, we describe the simple analytical model that could be used to estimate the inflow into the tunnel. This approach corresponds to the model introduced in Fig. 2b.

The Bernoulli theorem expresses the conservation of energy in a system: the sum of kinetic and potential energy should remain constant in the system. This supposes that the flow is in a steady-state, that the fluid is incompressible, and that the viscous and thermal effects are neglected. The Bernoulli expression between a point i at the entrance of a karst conduit and j where the conduit flows into the tunnel takes the following form:

$$\frac{v_i^2}{2g} + z_i + \frac{P_i}{\rho g} = \frac{v_j^2}{2g} + z_j + \frac{P_j}{\rho g} + \Delta H, \tag{4}$$

ΔH represents the head loss between the two points, v is the velocity, g is the gravitational acceleration, P the pressure, and z the elevation. If we consider that the atmospheric pressure is identical on both sides, that the velocity at the origin point is negligible compared to the outflow one, and that the difference in height is comparable to the hydraulic head gradient, we can simplify the equation as:

$$h = \frac{v_j^2}{2g} + \Delta H, \tag{5}$$

where h is the hydraulic head gradient equal to $h = z_i - z_j$.

If we neglect the head loss at the entrance of the conduit, the head loss ΔH along the conduit can be described by the Darcy–Weisbach Eq. (2), it then depends on the friction factor λ, and the length of the pipe L. The discharge can be estimated by solving a system of 2 equations: the combination of the Darcy–Weisbach Eq. (2) and the Bernoulli Eq. (5):

$$h - \frac{v^2}{2g}\left(1 + \frac{\lambda}{d}L\right) = 0, \tag{6}$$

and the Swamee Eq. (3).

If the diameter of the pipe is known, this system of equations can be solved to obtain the mean velocity and the discharge in the tunnel. But for a practical application in a complex karst network where the diameters are variable in space and not well known, it is not clear which diameter should be used in this formulation. Should one use the geometric mean of the local diameters for example?

To answer this question, we use the results of the numerical simulations and estimate the equivalent diameter that allows estimating properly the discharge and represents the complex karst system in a simpler manner. To compute the equivalent diameter, we use the value of the velocity computed with *DisCo* and solve Eq. (6) conjointly with the Swamee Eq. (3) using a Least Square minimization scheme.

3. Results

3.1. General comments

Fig. 8 shows two examples of simulated pressure fields, one for each karst scenario, associated with their karstic conduit network and the tunnel location in the corresponding simulation. The main pressure drops are observed around the tunnel, or around densely connected zones linked to the tunnel. The pressure diffusion appears to be mainly controlled by the karst conduit diameters. We can also observe that the pressure drop is irregularly distributed around the tunnel. Some parts of the network, connected to the tunnel, are less influenced by the pressure drop than other branches. This can be explained by the presence of small conduit apertures along these branches, reducing the possibility that the pressure drop propagates effectively. *Case 1* in Fig. 8 is a good example of such limitation of propagation. The matrix pressure drop is clearly asymmetrical between the left and the right size of the tunnel position. However, Fig. 9 *Case 1* shows that the karst conduit connected to the tunnel is getting much smaller towards the left. These smaller sections clearly delimit the pressure drop in the conduits, and also limit the pressure change in the matrix. On the other hand, the right side of the conduit has no limiting diameter and therefore shows an efficient matrix drainage and pressure diffusion.

Regarding the matrix, it is only influenced near the well-connected structures influenced by the pressure drop and linked to the tunnel breach location. The connectivity (conduit's aperture continuity along a branch) and density of the conduit are the main parameters controlling the pressure field diffusion.

We also analyzed the influence of the tunnel location on both the x and z axes on the long-term inflow (Fig. 10). These figures show that the locations of the tunnel have a modest influence on the possible inflow. Only a weak increase of the mean discharge value is observable when increasing the pressure gradient (moving up on the z coordinate), while no particular relation appears between the flow values and the x axis coordinate. As a consequence, the distance between the tunnel and the paleo-outlet (located at $x = 0$ m, $y = 55$ m and $z = 0$ m) does not appear to influence significantly the inflow values and is not considered as a main parameter controlling the system. The breach diameter (i.e: the size of the conduit in contact with the tunnel) also does not show a clear influence on the flow values. It appears that the geometry of the complex karstic conduit network limits the amount of water available at the breach, making the section not limiting.

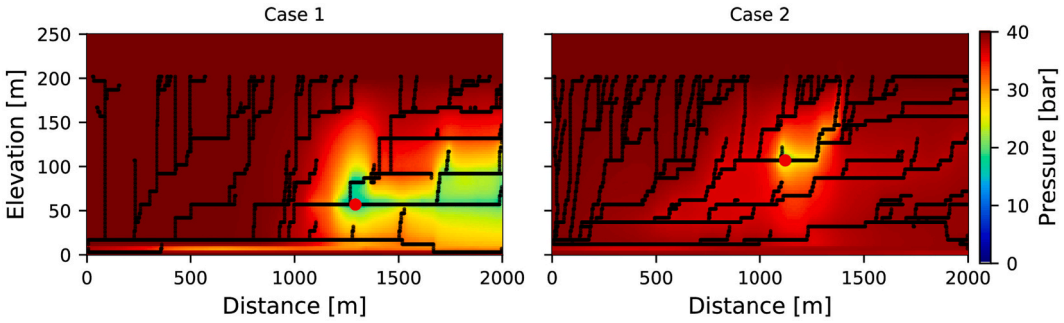

Fig. 8. Simulated pressure fields for both karst scenarios. The main pressure drops are located along karst conduits that are well developed and connect the tunnel breach location with the recharge area on the top of the domain. Resulting flows for these two models are 46 l/s for *Case 1*, and 117 l/s for *Case 2*.

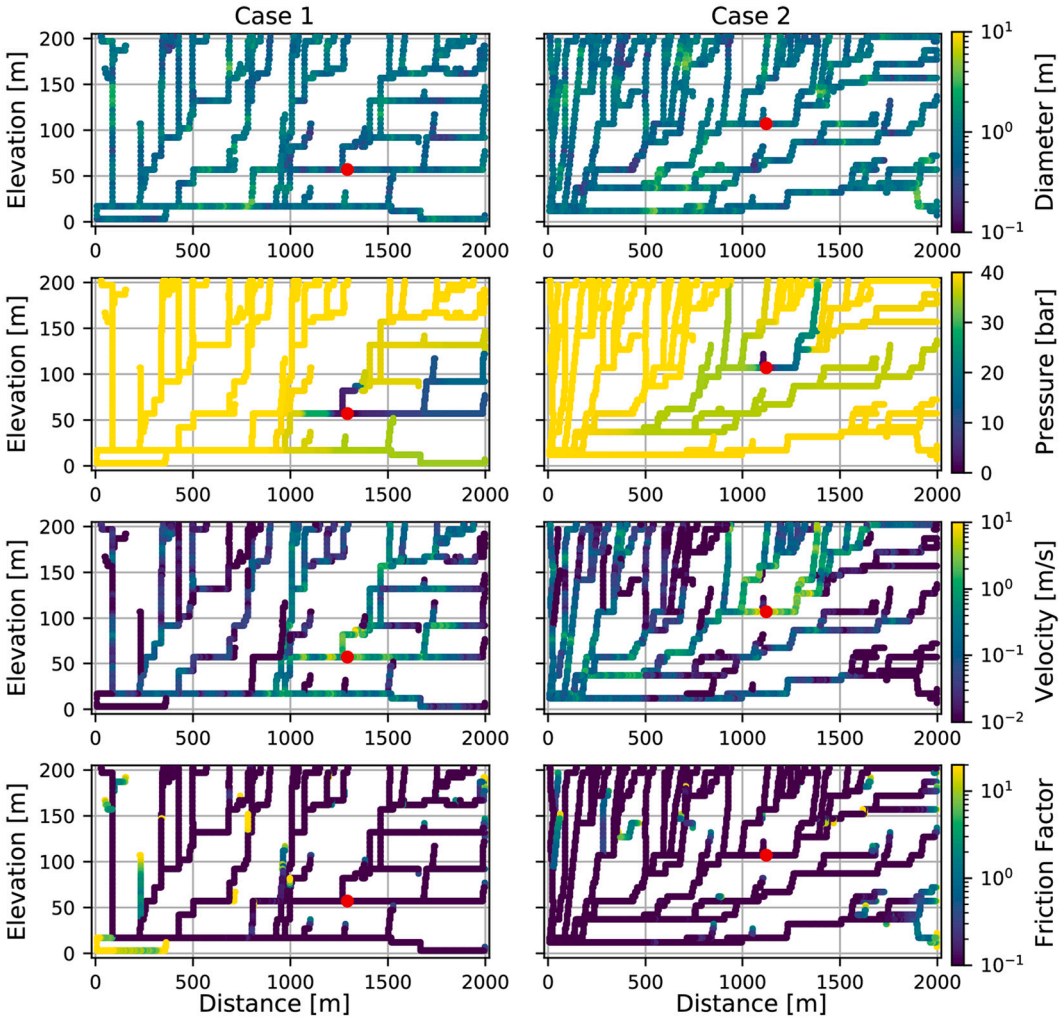

Fig. 9. Examples of model outputs displayed on the karstic conduit networks. The conduits aperture drives the diffusion of the pressure field and is linked to the output velocity values. The friction coefficient is less influenced by the connectivity of the network, only the dead ends of the karstic conduit network are showing a large value, while the rest of the system is more homogeneously distributed. Resulting flows for these two models are 46 l/s for *Case 1*, and 117 l/s for *Case 2*.

3.2. Influence of pressure difference

Using the ensemble of realizations, it is possible to statistically analyze the influence of the pressure difference on the long-term inflow at the tunnel breach location. The distribution of the possible inflow is presented in Table 3 and shows values ranging from 9.9 to 869.4 l/s for pressure difference ranging from 35 to 50 bar. The mean value of the 4 tested pressure difference simulation sets are ranging from 106.0 to 138.4 l/s. The cumulative distribution presented in Fig. 11, shows the linear influence of the pressure difference on the output flow of the system. The cumulative density functions (cdf) show a Gaussian-like shape. These cdfs are useful to directly analyze the probability of a specified flow value to occur, regarding the defined conceptual setting. Here, in more than 50% of the tested scenarios, the long-term flow encountered in the breached karst conduit does not go above 100 l/s, which can give essential information during the planning phase of the project (Fig. 11).

While the initial flow bursting out of the conduits is directly linked to the aperture of the breach, it is not the case for the long-term flow, which depends on the entire karstic conduit network connectivity and on the matrix/conduits relationship. Fig. 12 shows that the estimated long-term inflow is not correlated significantly with the karst conduit section aperture hit by the tunnel. The long-term inflow is controlled globally on the one hand by the whole structure of the conduit network, between the tunnel and top of the limestone formation, and on the other hand by the distribution of the conduit diameters. For a scenario with a pressure difference of 40 bar the mean value goes from 114.7 l/s for the karst *Case 1* to 121.3 l/s for the karst *Case 2*, while the maximal value of the sets passe from 758.5 l/s for the *Case 1* to 723.2 l/s for the denser *Case 2*.

3.3. Influence of matrix conductivity

The matrix directly feeds the karst conduits and can have an important impact on the resulting tunnel inflow value. Indeed, when increasing the equivalent hydraulic conductivity of the matrix, the mean value of the flow also increases. Five series of 120 simulations were conducted with a pressure difference of 40 bar and different hydraulic conductivities were tested. Table 4 summarizes these results and shows the influence of the matrix hydraulic conductivity on the discharge flow values to the tunnel. The results are not separated between Cases 1 and 2 since the same behavior as described in Table 3, with a slight tendency to obtain higher flows with the denser karst scenario (*Case 2*). With a two-order of magnitude increase in hydraulic conductivity, the mean flow value goes from 112.9 l/s to 436 l/s. When a karst conduit flow is limited, due to poor connection within the conduit network, the exchange between the conduits and the matrix can play a major role and strongly impact the inflow produced at the tunnel breach location.

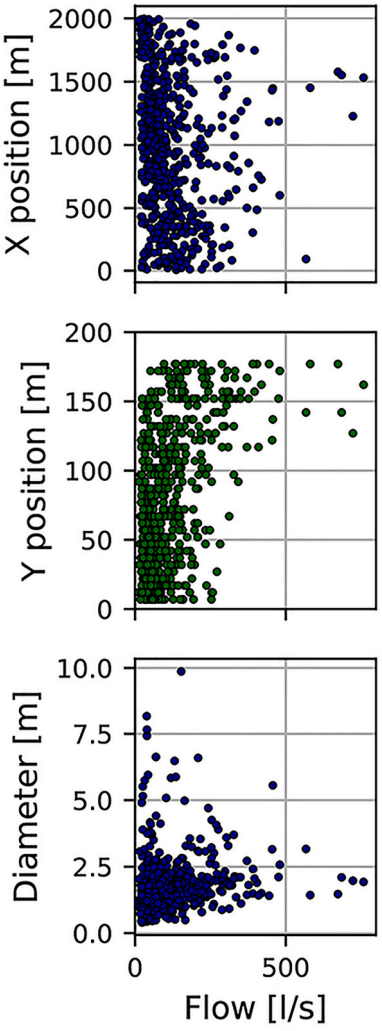

Fig. 10. Relation between the calculated outflow and the tunnel location for the 40 bar scenario. The two types of karst geometries (Cases 1 and 2) are shown together here.

Table 3
Statistics of the calculated permanent inflow as a function of pressure differences and types of network structure (Case type).

		Flow [l/s]			
ΔPressure [bar]	Case	Minimum	Median	Mean	Maximum
35	1	9.9	81.7	106.0	698.3
35	2	12.2	77.5	112.0	670.1
40	1	10.7	88.5	114.7	758.5
40	2	13.3	84.2	121.3	723.2
45	1	11.5	95.0	123.0	815.3
45	2	14.3	91.3	130.1	773.2
50	1	12.3	101.4	131.0	869.4
50	2	15.4	98.0	138.4	820.7

3.4. Friction factor analysis

In this section, we analyze the friction factor values calculated in the conduits for the long-term flow estimation. The statistics of the friction factors, calculated with the Swamee (1993) approach during the simulations, are presented in Table 5 and show values ranging from 0.018 to 850. These values are not significantly influenced by the pressure difference prescribed in the system because instead they are mainly controlled by the specific roughness and the conduit diameters, which

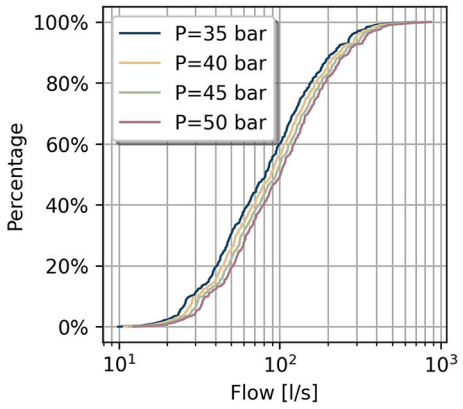

Fig. 11. Long-term cumulative density functions of the four pressure difference test sets. The results encompass both of the two karst scenarios.

are respectively fixed, and follow the same statistical distribution for all the simulations.

It is interesting to compare the distribution of the calculated friction factor to the one gathered by Herman et al. (2012). It appears that the mean values presented in Table 5 are closer to the friction factor derived from roughness estimation, ranging from 0.039 to 0.9 in Herman et al. (2012). This is expected since the friction factor are locally calculated in our simulations. We also encounter a few exceptional extreme values (Table 5) but they occur when the velocity values came close to zero, near to some dead-ends of the networks (Fig. 9). The friction factors calculated from discharge measurements in the field range from 0.116 to 340 in Herman et al. (2012). These friction factors generally represent equivalent values that encompass the entire domain, without taking into account the specific geometry of the network.

3.5. Single pipe equivalent

Finally, for all the simulations and their associated tunnel locations, an equivalent pipe diameter is estimated as described in Section 2.6. Fig. 13 shows the resulting calculated diameters compared to the geometric mean of the diameters of the conduits surrounding the tunnel in a 60 m radius. We observe that the single pipe equivalent diameters are at least one order of magnitude smaller than the geometric means. A general trend is visible in the results, with a slight positive correlation, but the relationship between equivalent pipe diameter and the geometric mean is very dispersed. Since all other parameters (relative rugosity, pressure gradient, and tunnel location) are kept unchanged, and since a straight path is considered in the analytical solution, the effect of the complex geometry of the network is entirely reflected in the equivalent diameter. In addition, we also analyzed the dependency of the equivalent diameter with the pressure range and did not observe any significant effect.

To conclude that analysis, using a single pipe equivalent approach can be applied, but further research is needed to develop efficient ways to estimate the equivalent diameter. Using simply the geometric mean of the conduit diameters in the surrounding of the tunnel leads to an important overestimation of the flow.

4. Discussion

This study presents a stochastic methodology for the estimation of the inflows that could be encountered during the construction of a tunnel intersecting a karstic conduit network. The originality of the approach is to combine three aspects: the SKS pseudo-genetic approach (Borghi et al., 2012; Fandel et al., 2021), used to simulate rapidly and efficiently a broad set of karst network geometries, a geostatistical simulation of the conduit diameters, and a physically-based model

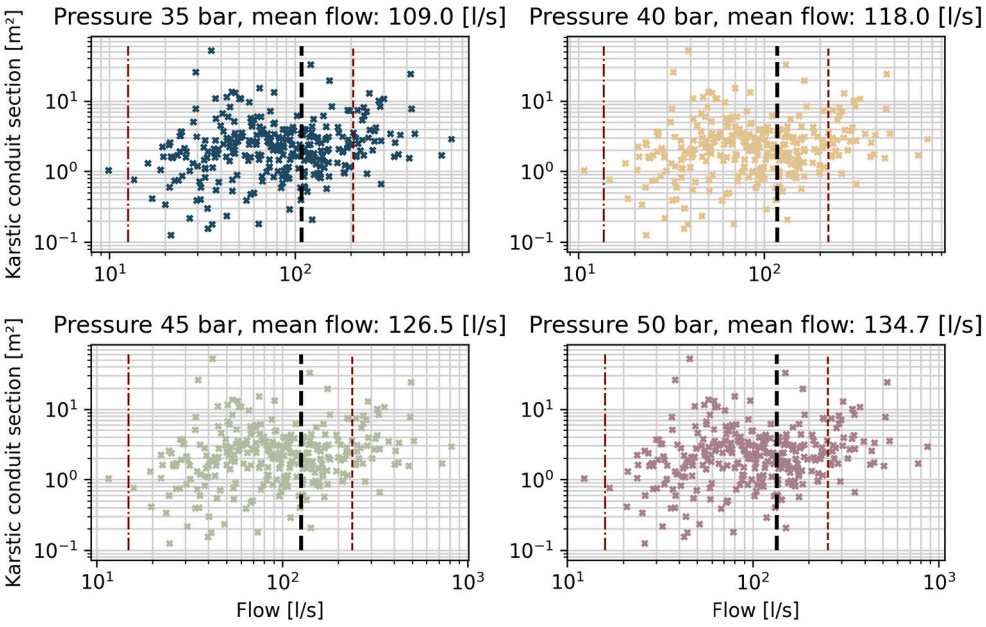

Fig. 12. Relation between the estimated long-term flow and the karst conduit section at the location of the tunnel. The black dot line representing the mean flow value and the red dot line the +/− one sigma standard deviation of the distribution.

Table 4
Statistics for permanent inflow calculation regarding the matrix hydraulic conductivity test sets. The two karst scenarios are grouped in this analysis.

	Flow [l/s]			
Hydraulic conductivity [m/s]	**Minimum**	**Median**	**Mean**	**Maximum**
$1{\cdot}10^{-7}$	17.8	85.7	112.9	390.6
$5{\cdot}10^{-7}$	29.8	126.1	150.3	406.0
$1{\cdot}10^{-6}$	32.9	162.6	181.7	459.7
$5{\cdot}10^{-6}$	45.5	318.3	325.4	719.0
$1{\cdot}10^{-5}$	55.0	423.6	436.0	1'100.2

Table 5
Statistics of the friction factor coefficient calculated from 100 simulations for each set of pressure gradient (the extremes values produced by numerical artifacts are removed).

	Friction factor λ [–]			
ΔPressure [bar]	**Minimum**	**Median value**	**Mean**	**Maximum**
35	0.018	0.045	1.69	850
40	0.018	0.045	1.57	799
45	0.018	0.044	1.41	712
50	0.018	0.044	1.27	622

capable of simulating groundwater flow in the conduits and the interactions with a permeable matrix (De Rooij et al., 2013; De Rooij, 2019). We argue that this workflow should allow obtaining reliable estimates of the statistical distribution of possible inflow rates in tunnels.

To check if the orders of magnitude of our results are reasonable, we compared the discharges calculated in this work with those of the existing literature. Only a few examples of simulations using realistic conduit networks and where the estimated flow rates are associated to specific conduits diameter were found. Jeannin et al. (2015) considered conduit's diameter distributions ranging from 0.2 to 2 m and provide flow estimates ranging from 10 to 10'000 l/s. Li et al. (2016) and Kang et al. (2019) study potential or historical water inrush during tunnel construction. Li et al. (2016) makes a list of historical events of water irruption and their associated volume of water ranges from 5.10^4 to

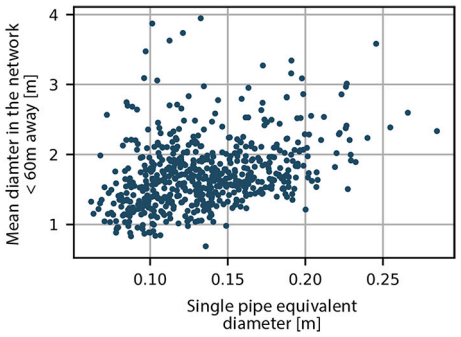

Fig. 13. Geometric mean of the karst conduits diameters in a 60 m radius to the tunnel and associated pipe equivalent diameter.

1.10^6 m^3 during an unknown time range. Li et al. (2016) also report events of water inrush during tunnel construction, having flow rates ranging from 530 to almost 2'000 l/s. Finally, Kang et al. (2019) study the dynamic of water inflow during tunnel excavation in karstified rock mass and calculate the average monthly water inflows monitored at both tunnel entrances during the excavation process over a 4 months period. The obtained flow rates are ranging from 50 to 140 l/s. No statement is made about any remediation work that could have been performed during the excavation operation. This brief literature overview demonstrates that our long-term inflow simulations, with our estimated permanent inflow ranging from 10 l/s to 820 l/s, are reasonable for the proposed conceptual model.

This comparison corroborates our statement that the proposed Monte-Carlo approach should enable its users to make proper risk assessments not only for tunnel projects but also for any underground or surface construction (dams for example) that may be threatened by massive flows related to karstic features.

Let us also emphasize that the proposed workflow can be used in different phases of the project. In the very early phase, one can use this approach to investigate the risks related to various scenarios under simplified geometries based only on some very general knowledge as illustrated with the example described in this paper. When more specific information are available, either about the geological or

hydrogeological context, the proposed approach can easily integrate additional data. On the one hand, for a specific site, the model geometry and mesh could follow the known topography and 3D geological structure of the study area. The construction of stochastic karst network models with SKS is capable to account for very realistic and complex geometries in 3D (Borghi et al., 2012) as well as a very wide range of situations, from alpine settings (Sivelle et al., 2020; Fandel et al., 2020) to coastal karstic environments (Vuilleumier et al., 2013), while possibly accounting for multiple phases of karstification (Banusch et al., 2022). On the other hand, *DisCo* is capable of handling complex aquifer and boundary conditions (De Rooij and Graham, 2017; De Rooij, 2019). *DisCo* can easily integrate additional information for example about the recharge distribution, the presence of springs, rivers, or lakes in the surface. These types of boundary conditions could be applied if the karstic formation would not be confined below a large aquifer as studied in this paper. Furthermore, *DisCo* can be employed both in steady or transient regime to analyze not only the long-term risks but also the early stages of water burst, the evolution of water inflows during the drilling phase of the tunnel or the seasonal fluctuations.

Despite these strengths, several aspects of the methodology can still be improved. For instance, more realistic techniques could be used to assign the conduit's diameters. It is possible to spatially correlate conduit diameters using curvilinear distances following the karst network instead of using an Euclidean distance in the geostatistical simulation algorithm as it was done by Frantz et al. (2021). Similarly, more realistic simulations of the heterogeneity of the matrix could be implemented based on conceptual models of the geological heterogeneity in carbonate formations (Petrovic et al., 2018). It would also be straightforward to compute spatially variable equivalent permeability tensors based on the discrete fracture networks simulated in the initial phase of the karst network simulation to ensure a better consistency between the matrix properties and the karst simulations. All these aspects may improve the realism of the simulations.

However, the most important limitation is that we did not show in this paper how to infer the statistical and physical parameters which control the uncertainty quantification from field observations and prior information. This question is not specific to the proposed workflow. As for any modeling exercise, there is a need to collect as much information as possible to constrain the model with reasonable parameters. Here, information on the fracture network can be derived from field measurements in outcrops or boreholes. The geometry of the aquifer can be derived from classical geological survey and 3D geological modeling techniques (Wellmann and Caumon, 2018). The hydrogeological boundary conditions can also be derived from standard hydrogeological reasoning and field data. Finally, the unknown parameters will need to be identified (model calibration) by comparing the predictions made with the model with measurements of state variables such as spring discharges, groundwater levels, or tracer data. Solving this inverse problem is likely to be difficult because the data are often scarce and because the response of the model will be stochastic and will depend both on the structure of the karst network, and its interaction with the petrophysical parameters and the boundary conditions. However, several methods exists and have already been employed in the framework of stochastic karst models (Borghi et al., 2016; Fischer et al., 2018; Fandel et al., 2020) and could be implemented within the proposed workflow. These methods would allow the model to be consistent with field observations.

Beyond the proposed methodology, the numerical study presented in this paper showed that the friction factors at the local scale remain small, with median values around 0.045 and mean values around 1.5, in general and much lower than the published values estimated globally from discharge measurements (Atkinson, 1977; Smart, 1988; Worthington, 1991).

Finally, we also show that it is theoretically possible to use a simple analytical solution (the single pipe model) to estimate the discharge in the tunnel and conduct a very rapid uncertainty analysis. But, the difficulty to follow this alternative approach is to find an efficient way to estimate the equivalent pipe diameter without having to solve the complex 3D flow problem. We consider this issue an interesting avenue for further research.

5. Conclusion

The main results obtained in this paper are as follows:

1. We propose to efficiently predict the probability distribution of potential water inflow in tunnels in karstic environments using a Monte-Carlo approach that couples a pseudo-genetic karstic conduit network generator and physically-based discrete–continuum flow simulations.
2. The method has been illustrated on a simplified confined aquifer situation and produced results that compare well with previously published values.
3. For the simple confined karstic aquifer studied in this paper, we predicted the long term steady-state water inflow after construction, and showed that it is mainly influenced by the pressure gradient and the dimension of the conduits around the breach location, rather than the diameter of the encountered conduit itself.
4. Even if the permeability of the limestone matrix is small, we showed that its value can have a significant effect on the predicted flows.
5. Using simpler single-pipe models to estimate flows is a promising approach. However, further work is needed to identify the proper way of estimating the equivalent diameter of complex karst networks.
6. Assuming that the required information is available, an estimate of inflow with an uncertainty estimation can be obtained within a few days. Performing such an analysis before the construction of underground structures in limestone should help defining risks and sizing emergency equipment for the actual execution of the civil engineering work.
7. In general, the proposed stochastic approach is versatile. It can be adapted to more complex geometries and hydrogeological conditions because the two numerical codes employed in that study can account for more realistic scenarios. However, one of the practical challenge in that perspective will be the identification of all the parameters of the model by solving an inverse problem.

CRediT authorship contribution statement

Valentin Dall'Alba: Conceptualization, Methodology, Software, Writing - original draft, Writing - review & editing. **Alexis Neven:** Conceptualization, Methodology, Software, Writing - original draft, Writing - review & editing. **Rob de Rooij:** Software, Writing – review & editing. **Marco Filipponi:** Conceptualization, Methodology, Writing – review & editing. **Philippe Renard:** Conceptualization, Methodology, Supervision, Writing - review & editing.

Declaration of Competing Interest

The authors declare that they have no known competing financial interests or personal relationships that could have appeared to influence the work reported in this paper.

Data availability

No data was used for the research described in the article.

Acknowledgments

The authors would like to thank the National Cooperative for the Disposal of Radioactive Waste (NAGRA) for its financial support. We also thank two anonymous reviewers who provided constructive

comments which helped improve the paper.

References

Atkinson, T., 1977. Diffuse flow and conduit flow in limestone terrain in the Mendip Hills, Somerset (Great Britain). J. Hydrol. 35, 93–110. https://doi.org/10.1016/0022-1694(77)90079-8.

Banusch, S., Somogyvári, M., Sauter, M., Renard, P., Engelhardt, I., 2022. Stochastic modeling approach to identify uncertainties of karst conduit networks in carbonate aquifers. Water Resour. Res. 58, e2021WR031710 https://doi.org/10.1029/2021WR031710. URL:https://agupubs.onlinelibrary.wiley.com/doi/abs/10.1029/2021WR031710.arXiv:https://agupubs.onlinelibrary.wiley.com/doi/pdf/10.1029/2021WR031710. E2021WR031710 2021WR031710.

Borghi, A., Renard, P., Jenni, S., 2012. A pseudo-genetic stochastic model to generate karstic networks. J. Hydrol. 414–415, 516–529. https://doi.org/10.1016/j.jhydrol.2011.11.032.

Borghi, A., Renard, P., Cornaton, F., 2016. Can one identify karst conduit networks geometry and properties from hydraulic and tracer test data? Adv. Water Resour. 90, 99–115. https://doi.org/10.1016/j.advwatres.2016.02.009.

Butscher, C., 2012. Steady-state groundwater inflow into a circular tunnel. Tunn. Undergr. Space Technol. 32, 158–167. https://doi.org/10.1016/j.tust.2012.06.007.

Çengel, Y.A., Cimbala, J.M., 2017. Fluid Mechanics: Fundamentals And Applications, 4th edition. McGraw-Hill Education, New York.

Chisyaki, T., 1984. A study on confined flow of ground water through a tunnel. Ground Water 22, 162–167. https://doi.org/10.1111/j.1745-6584.1984.tb01485.x.

Day, M.J., 2004. Karstic problems in the construction of milwaukee's deep tunnels. Environ. Geol. 45, 859–863. https://doi.org/10.1007/s00254-003-0945-4.

De Rooij, R., 2019. Improving accuracy and efficiency in discrete-continuum karst models. Environ. Earth Sci. 78 https://doi.org/10.1007/s12665-019-8115-5.

De Rooij, R., Graham, W., 2017. Generation of complex karstic conduit networks with a hydrochemical model. Water Resour. Res. 53, 6993–7011. https://doi.org/10.1002/2017wr020768.

De Rooij, R., Perrochet, P., Graham, W., 2013. From rainfall to spring discharge: Coupling conduit flow, subsurface matrix flow and surface flow in karst systems using a discrete continuum model. Adv. Water Resour. 61, 29–41. https://doi.org/10.1016/j.advwatres.2013.08.009.

Deutsch, C.V., Journel, A.G., et al., 1992. Geostatistical software library and user's guide. New York, 119.

El Tani, M., 2003. Circular tunnel in a semi-infinite aquifer. Tunn. Undergr. Space Technol. 18, 49–55. https://doi.org/10.1016/s0886-7798(02)00102-5.

Fandel, C., Ferré, Ty, Chen, Z., Renard, P., Goldscheider, N., 2020. A model ensemble generator to explore structural uncertainty in karst systems with unmapped conduits. Hydrogeol. J. 29, 229–248. https://doi.org/10.1007/s10040-020-02227-6.

Fandel, C., Miville, F., Ferré, T., Goldscheider, N., Renard, P., 2021. The stochastic simulation of karst conduit network structure using anisotropic fast marching, and its application to a geologically complex alpine karst system. Hydrogeol. J. In review.

Filipponi, M., Jeannin, P.-Y., 2010. Karst-alea: a scientific based karst risk assessment for underground engineering. In: Andreo, B., Carrasco, F., Dūran, J., LaMoreaux, J. (Eds.), Advances in Research in Karst Media. Springer, pp. 435–440. https://doi.org/10.1007/978-3-642-12486-0_67.

Filipponi, M., Jeannin, P.-Y., Tacher, L., 2009. Evidence of inception horizons in karst conduit networks. Geomorphology 106, 86–99. https://doi.org/10.1016/j.geomorph.2008.09.010.

Fischer, P., Jardani, A., Lecoq, N., 2018. Hydraulic tomography of discrete networks of conduits and fractures in a karstic aquifer by using a deterministic inversion algorithm. Adv. Water Resour. 112, 83–94. https://doi.org/10.1016/j.advwatres.2017.11.029.

Ford, D., Williams, P.D., 2007. Karst hydrogeology and geomorphology. John Wiley & Sons. https://doi.org/10.1002/9781118684986.

Frantz, Y., Collon, P., Renard, P., Viseur, S., 2021. Analysis and stochastic simulation of geometrical properties of conduits in karstic networks. Geomorphology 377, 107480. https://doi.org/10.1016/j.geomorph.2020.107480.

Gangrade, R.M., Grasmick, J.G., Mooney, M.A., 2021. Probabilistic assessment of void risk and grouting volume for tunneling applications. Rock Mech. Rock Eng. https://doi.org/10.1007/s00603-021-02528-6.

Goldscheider, N., Drew, D. (Eds.), 2014. Methods in Karst Hydrogeology. CRC Press. https://doi.org/10.1201/9781482266023.

Gutiérrez, F., Parise, M., Waele, J.D., Jourde, H., 2014. A review on natural and human-induced geohazards and impacts in karst. Earth Sci. Rev. 138, 61–88. https://doi.org/10.1016/j.earscirev.2014.08.002.

He, B., 2015. Numerical simulation analysis of karst tunnel water bursting movement, pp. 668–676. doi:10.2991/iccet-15.2015.125.

Herman, E.K., Toran, L., White, W.B., 2012. Clastic sediment transport and storage in fluviokarst aquifers: an essential component of karst hydrogeology. Carbonates Evaporites 27, 211–241. https://doi.org/10.1007/s13146-012-0112-7.

Hwang, J.-H., Lu, C.-C., 2007. A semi-analytical method for analyzing the tunnel water inflow. Tunn. Undergr. Space Technol. 22, 39–46. https://doi.org/10.1016/j.tust.2006.03.003.

Jaquet, O., Siegel, P., Klubertanz, G., Benabderrhamane, H., 2004. Stochastic discrete model of karstic networks. Adv. Water Resour. 27, 751–760. https://doi.org/10.1016/j.advwatres.2004.03.007.

Javadi, M., Sharifzadeh, M., Shahriar, K., 2016. Uncertainty analysis of groundwater inflow into underground excavations by stochastic discontinuum method: Case study of siah bisheh pumped storage project, iran. Tunn. Undergr. Space Technol. 51, 424–438. https://doi.org/10.1016/j.tust.2015.09.003.

Jeannin, P.-Y., Malard, A., Rickerl, D., Weber, E., 2015. Assessing karst-hydraulic hazards in tunneling—the brunnmühle spring system—bernese jura, switzerland. Environ. Earth Sci. 74, 7655–7670. https://doi.org/10.1007/s12665-015-4655-5.

Jiang, C., Han, H., Xie, H., Liu, J., Chen, Z., Chen, H., 2021. Karst aquifer water inflow into tunnels: an analytical solution. Geofluids 2021, 1–10. https://doi.org/10.1155/2021/6672878.

Kang, X., Luo, S., Xu, M., Zhang, Q., Yang, Y., 2019. Dynamic estimating the karst tunnel water inflow based on monitoring data during excavation. Acta Carsologica 48. https://doi.org/10.3986/ac.v48i1.4654.

Király, L., et al., 1976. Etude de la régularisation de l'areuse par modèle mathématique. Bulletin du Centre d'Hydrogéologie 1, 19–36.

Király, L., 1988. Large scale 3-D groundwater flow modelling in highly heterogeneous geologic medium. Springer. https://doi.org/10.1007/978-94-009-2889-3_38.

Kresic, N., Panday, S., 2018. Numerical groundwater modelling in karst. Geol. Soci. Lond. Spec. Publ. 466, 319–330. https://doi.org/10.1144/sp466.12.

Lee, S., Moon, J.-S., 2020. Excessive groundwater inflow during tbm tunneling in limestone formation. Tunn. Undergr. Space Technol. 96, 103217 https://doi.org/10.1016/j.tust.2019.103217.

Li, S.-C., Zhou, Z.-Q., Li, L.-P., Xu, Z.-H., Zhang, Q.-Q., Shi, S.-S., 2013. Risk assessment of water inrush in karst tunnels based on attribute synthetic evaluation system. Tunn. Undergr. Space Technol. 38, 50–58. https://doi.org/10.1016/j.tust.2013.05.001.

Li, L., Tu, W., Shi, S., Chen, J., Zhang, Y., 2016. Mechanism of water inrush in tunnel construction in karst area. Geomat. Nat. Hazards Risk 7, 35–46. https://doi.org/10.1080/19475705.2016.1181342.

Li, J., Hong, A., Yuan, D., Jiang, Y., Deng, S., Cao, C., Liu, J., 2021. A new distributed karst-tunnel hydrological model and tunnel hydrological effect simulations. J. Hydrol. 593, 125639 https://doi.org/10.1016/j.jhydrol.2020.125639.

Lin, C., Zhang, M., Zhou, Z., Li, L., Shi, S., Chen, Y., Dai, W., 2020. A new quantitative method for risk assessment of water inrush in karst tunnels based on variable weight function and improved cloud model. Tunn. Undergr. Space Technol. 95, 103136 https://doi.org/10.1016/j.tust.2019.103136.

Liu, J., Shen, L., Wang, Z., Duan, S., Wu, W., Peng, X., Wu, C., Jiang, Y., 2019. Response of plants water uptake patterns to tunnels excavation based on stable isotopes in a karst trough valley. J. Hydrol. 571, 485–493. https://doi.org/10.1016/j.jhydrol.2019.01.073.

Lowe, D., Gunn, J., 1997. Carbonate speleogenesis: an inception horizon hypothesis. Acta Carsologica 26, 457–488.

Luo, M., Chen, J., Jakada, H., Li, N., Guo, X., Zhou, H., 2022. Identifying and predicting karst water inrush in a deep tunnel, South China. Eng. Geol. 106716. https://doi.org/10.1016/j.enggeo.2022.106716.

Lv, Y., Jiang, Y., Hu, W., Cao, M., Mao, Y., 2020. A review of the effects of tunnel excavation on the hydrology, ecology, and environment in karst areas: current status, challenges, and perspectives. J. Hydrol. 586, 124891 https://doi.org/10.1016/j.jhydrol.2020.124891.

Maleki, M.R., 2018. Groundwater seepage rate (gsr); a new method for prediction of groundwater inflow into jointed rock tunnels. Tunn. Undergr. Space Technol. 71, 505–517. https://doi.org/10.1016/j.tust.2017.10.006.

Maréchal, J.-C., Lanini, S., Aunay, B., Perrochet, P., 2014. Analytical solution for modeling discharge into a tunnel drilled in a heterogeneous unconfined aquifer. Groundwater 52, 597–605. https://doi.org/10.1111/gwat.12087.

Miville, F., 2019. Modélisation stochastique du bassin versant karstique de la source du Betteraz (JU). Master's thesis. Université de Neuchâtel, Centre for Hydrogeology and Geothermics Switzerland.

Panday, S., Huyakorn, P.S., 2004. A fully coupled physically-based spatially-distributed model for evaluating surface/subsurface flow. Adv. Water Resour. 27, 361–382. https://doi.org/10.1016/j.advwatres.2004.02.016.

Pardo-Iguzquiza, E., Duràn-Valsero, J.J., Rodríguez-Galiano, V., 2011. Morphometric analysis of three-dimensional networks of karst conduits. Geomorphology 132, 17–28. https://doi.org/10.1016/j.geomorph.2011.04.030.

Pardo-Igúzquiza, E., Dowd, P.A., Xu, C., Durán-Valsero, J.J., 2012. Stochastic simulation of karst conduit networks. Adv. Water Resour. 35, 141–150. https://doi.org/10.1016/j.advwatres.2011.09.014.

Park, Y.-J., Hwang, H.-T., Suzuki, S., Saegusa, H., Nojiri, K., Tanaka, T., Bruines, P., Abumi, K., Morita, Y., Illman, W., 2020. Improving precision in regional scale numerical simulations of groundwater flow into underground openings. Eng. Geol. 274, 105727 https://doi.org/10.1016/j.enggeo.2020.105727.

Perrochet, P., 2005. A simple solution to tunnel or well discharge under constant drawdown. Hydrogeol. J. 13, 886–888. https://doi.org/10.1007/s10040-004-0355-z.

Petrovic, A., Aigner, T., Pontiggia, M., 2018. Facies heterogeneities in a ramp carbonate reservoir analogue: a new high-resolution approach for 3d facies modelling. J. Pet. Geol. 41, 155–174. https://doi.org/10.1111/jpg.12698.

Raymer, J., 2005. Groundwater inflow into hard rock tunnels: a new look at inflow equations. In: Rapid Excavation and Tunneling Conference, pp. 457–468.

Reimann, T., Geyer, T., Shoemaker, W.B., Liedl, R., Sauter, M., 2011. Effects of dynamically variable saturation and matrix-conduit coupling of flow in karst aquifers. Water Resour. Res. 47 https://doi.org/10.1029/2011wr010446.

Renard, P., 2005. Approximate discharge for constant head test with recharging boundary. Groundwater 43, 439–442. https://doi.org/10.1111/j.1745-6584.2005.0024.x.

Scheidler, S., Huggenberger, P., Butscher, C., Dresmann, H., 2017. Tools to simulate changes in hydraulic flow systems in complex geologic settings affected by tunnel excavation. Bull. Eng. Geol. Environ. 78, 969–980. https://doi.org/10.1007/s10064-017-1113-5.

Sedghi, M.M., Zhan, H., 2021. On inflow to a tunnel in a fractured double-porosity aquifer. Groundwater 59, 562–570. https://doi.org/10.1111/gwat.13079.
Sethian, J.A., 1996. A fast marching level set method for monotonically advancing fronts. Proc. Nat. Acad. Sci. 93, 1591–1595. https://doi.org/10.1073/pnas.93.4.1591.
Shoemaker, W.B., Kuniansky, E.L., Birk, S., Bauer, S., Swain, E.D., 2008. Documentation of a conduit flow process (cfp) for modflow-2005.
Sivelle, V., Renard, P., Labat, D., 2020. Coupling sks and swmm to solve the inverse problem based on artificial tracer tests in karstic aquifers. Water 12, 1139. https://doi.org/10.5194/egusphere-egu2020-10318.
Smart, C., 1988. Quantitative tracing of the Maligne karst system, Alberta, Canada. J. Hydrol. 98, 185–204. https://doi.org/10.1016/0022-1694(88)90014-5.
Song, K.-I., Cho, G.-C., Chang, S.-B., 2012. Identification, remediation, and analysis of karst sinkholes in the longest railroad tunnel in South Korea. Eng. Geol. 135, 92–105. https://doi.org/10.1016/j.enggeo.2012.02.018.
Swamee, P.K., 1993. Design of a submarine oil pipeline. J. Transp. Eng. 119, 159–170. https://doi.org/10.1061/(asce)0733-947x(1993)119:1(159).
Vincenzi, V., Gargini, A., Goldscheider, N., Piccinini, L., 2013. Differential hydrogeological effects of draining tunnels through the Northern Apennines, Italy. Rock Mech. Rock Eng. 47, 947–965. https://doi.org/10.1007/s00603-013-0378-7.
Vuilleumier, C., Borghi, A., Renard, P., Ottowitz, D., Schiller, A., Supper, R., Cornaton, F., 2013. A method for the stochastic modeling of karstic systems accounting for geophysical data: an example of application in the region of Tulum, Yucatan Peninsula (Mexico). Hydrogeol. J. 21, 529–544. https://doi.org/10.1007/s10040-012-0944-1.
Wellmann, F., Caumon, G., 2018. 3-d structural geological models: concepts, methods, and uncertainties. In: Adv. Geophys., vol. 59. Elsevier, pp. 1–121.
Worthington, S., 1991. Karst hydrogeology of the canadian rocky mountains. Ph.D. thesis. McMaster University, Hamilton. Ont., Can.
Xie, H.-S., Jiang, C., He, J.-L., Han, H.-X., 2019. Analytical solution for the steady-state karst water inflow into a tunnel. Geofluids 2019, 1–9. https://doi.org/10.1155/2019/1756856.